

# THE OPTICAL MODEL POTENTIAL OF THE $\Sigma$ HYPERON IN NUCLEAR MATTER\*

JANUSZ DĄBROWSKI, JACEK ROŻYNEK

Theoretical Physics Division, A. Sołtan Institute for Nuclear Studies  
Hoża 69, 00-681 Warsaw, Poland

*(Received December 1, 2009)*

We present our attempts to determine the optical model potential  $U_\Sigma = V_\Sigma - iW_\Sigma$  of the  $\Sigma$  hyperon in nuclear matter. We analyze the following sources of information on  $U_\Sigma$ :  $\Sigma N$  scattering,  $\Sigma^-$  atoms, and final state interaction of  $\Sigma$  hyperons in the  $(\pi, K^+)$  and  $(K^-, \pi)$  reactions on nuclear targets. We conclude that  $V_\Sigma$  is repulsive inside the nucleus and has a shallow attractive pocket at the nuclear surface. These features of  $V_\Sigma$  are consistent with the Nijmegen model F of the hyperon–nucleon interaction.

PACS numbers: 21.80.+a

## 1. Introduction

The interaction of the  $\Sigma$  hyperon with nuclear matter may be represented by the complex single particle (s.p.) optical model potential  $U_\Sigma = V_\Sigma - iW_\Sigma$ . In this paper we present our attempts to determine  $V_\Sigma$  and  $W_\Sigma$ . We also point out the most realistic two-body  $\Sigma N$  interaction among the available OBE models of the baryon–baryon interaction.

In the present paper we discuss the following sources of information on  $U_\Sigma$ :  $\Sigma N$  scattering data in Sec. 2,  $\Sigma^-$  atoms in Sec. 3, associated production reactions in Sec. 4, and strangeness exchange reactions in Sec. 5. Our conclusions are presented in Sec. 6.

## 2. $\Sigma N$ scattering

The way from the  $\Sigma N$  scattering data to  $U_\Sigma$  consists of two steps: first, we determine the two-body  $\Sigma N$  interaction  $\mathcal{V}_{\Sigma N}$ , and second, with this  $\mathcal{V}_{\Sigma N}$  we calculate  $U_\Sigma$ . The scarcity of the two-body  $\Sigma N$  data makes the first step very difficult. A way of overcoming these difficulties was followed

---

\* Presented at the XXXI Mazurian Lakes Conference on Physics, Piaski, Poland, August 30–September 5, 2009.

by de Swart and his collaborators in Nijmegen: they assumed the mechanism of one-boson exchange (OBE) and the SU(3) symmetry which enabled them to employ the numerous  $NN$  data in determining the parameters of their two-body interaction. In this way they produced a number of the Nijmegen models of the baryon–baryon interaction: models D [1], F [2], soft core (SC) model [3], and the new soft-core (NSC) model [4].

### 2.1. The real potential $V_\Sigma$

In calculating  $V_\Sigma$  we use the real part of the effective  $\Sigma N$  interaction YNG [5] in nuclear matter. The YNG interaction is the configuration space representation of the  $G$  matrix calculated in the low order Brueckner approximation with the Nijmegen models of the baryon–baryon interaction. Our results obtained for  $V_\Sigma$  as function of the nucleon density  $\rho$  are shown in Fig. 1. As the dependence of  $V_\Sigma$  on the  $\Sigma$  momentum  $k_\Sigma$  is not very

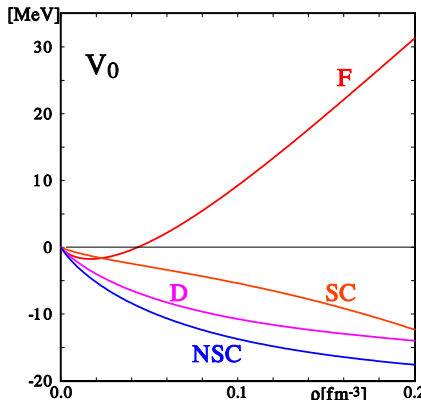


Fig. 1. The isoscalar potential  $V_\Sigma$  as a function of the nucleon density  $\rho$  at  $k_\Sigma = 0$  for the indicated Nijmegen models of the  $\Sigma N$  interaction.

strong in the relevant interval of  $k_\Sigma$  [6], we use for  $V_\Sigma$  its value calculated at  $k_\Sigma = 0$ . We see that all the Nijmegen interaction models, except for model F, lead to pure attractive  $V_\Sigma$  which implies the existence of bound states of  $\Sigma$  hyperons in the nuclear core, *i.e.*,  $\Sigma$  hypernuclei. Since no  $\Sigma$  hypernuclei have been observed<sup>1</sup>, we conclude that among the Nijmegen interaction models model F is the only realistic representation of the  $\Sigma N$  interaction.

<sup>1</sup> The observed bound state of  $^4\Sigma$ He [7] is an exception. In the theoretical description of this state, Harada and his collaborators [8] apply phenomenological  $\Sigma N$  interactions, in particular, the interaction SAP-F simulating at low energies the Nijmegen model F interaction. They show that essential for the existence of the bound state of  $^4\Sigma$ He is a strong Lane component  $V_\tau$  in  $V_\Sigma$ , and among the Nijmegen models the strongest  $V_\tau$  is implied by model F [9].

## 2.2. The absorptive potential $W_\Sigma$

As pointed out in [5], the imaginary part of the YNG interaction is very sensitive to the choice of the intermediate state energies in the  $G$  matrix equation. In this situation we decided to use for  $W_\Sigma$  the semi-classical expression in terms of the total cross-sections (modified by the exclusion principle) for  $\Sigma N$  scattering, described in [10]. We denote by  $W_c$  the contribution to the absorptive potential of the  $\Sigma\Lambda$  conversion process  $\Sigma N \rightarrow \Lambda N'$  and by  $W_e$  the contribution of the  $\Sigma N$  elastic scattering, and have  $W_\Sigma = W_t = W_c + W_e$ <sup>2</sup>.

Our results obtained for  $W_c, W_e, W_t$  for nuclear matter (with  $N = Z$ ) at equilibrium density  $\rho = \rho_0 = 0.166 \text{ fm}^{-3}$  are shown in Fig. 2. With increasing momentum  $k_\Sigma$  the  $\Sigma\Lambda$  conversion cross-section decreases, on the other hand the suppression of  $W_c$  by the exclusion principle weakens. As the net result  $W_c$  does not change very much with  $k_\Sigma$ . The same two mechanisms act in the case of  $W_e$ . Here, however, the action of the exclusion principle is much more pronounced: at  $k_\Sigma = 0$  the suppression of  $W_e$  is complete. At higher momenta, where the Pauli blocking is not important, the total elastic cross-section is much bigger than the conversion cross-section, and we have  $W_e \gg W_c$ , and consequently  $W_\Sigma \gg W_c$ .

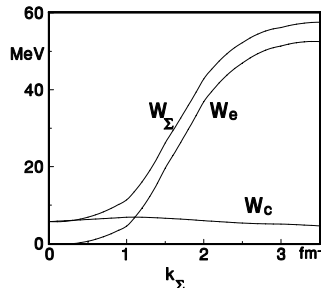


Fig. 2. The component  $W_c, W_e$ , and  $W_t$  of the  $\Sigma$  absorptive potential in nuclear matter of density  $\rho_0$  as functions of  $k_\Sigma$ .

## 3. $\Sigma^-$ atoms

The available data on strong interaction effects in  $\Sigma^-$  atoms consist of 23 data points: strong interaction shifts  $\varepsilon$  and widths  $\Gamma$  of the observed levels. These shifts and widths can be measured directly only in the lowest  $\Sigma^-$  atomic levels. The widths of the next to the last level can be obtained indirectly from measurements of the relative yields of X-rays.

<sup>2</sup> Notice that in the case of the nucleon optical potential in nuclear matter (for nucleon energies below the threshold for pion production),  $V_N - iW_N$ , only the elastic  $NN$  scattering contributes to  $W_N$ , and the situation is similar as in the case of the contribution  $W_e$  to  $W_\Sigma$ .

In [11], we have estimated the 23 values of  $\varepsilon$  and  $\Gamma$  from the difference between the eigenvalues of the Schrödinger equation of  $\Sigma^-$  in  $\Sigma^-$  atoms with the strong  $\Sigma^-$ -atomic nucleus interaction and without this interaction. To obtain this strong interaction, we applied the local density approximation, and used our optical model of Sec. 2. The agreement of our results, calculated with the optical potentials (obtained with the 4 Nijmegen  $\Sigma N$  interaction models) with the 23 empirical data points is characterized by the following values of  $\chi^2$ :  $\chi^2(\text{model D}) > 130$ ,  $\chi^2(\text{model F}) = 38.1$ ,  $\chi^2(\text{model SC}) = 55.0$ ,  $\chi^2(\text{model NSC}) > 904$ , and we conclude that the  $\Sigma^-$  atomic data point out at model F as the best representation of the  $\Sigma N$  interaction<sup>3</sup>.

#### 4. The associated production reactions

The first associated  $\Sigma$  production reaction ( $\pi^-, K^+$ ) was observed at KEK on  $^{28}\text{Si}$  target at pion momentum of 1.2 GeV/c ([12, 13]), and this reaction is the subject of the present analysis. We consider the reaction ( $\pi^-, K^+$ ) in which the pion  $\pi^-$  with momentum  $\mathbf{k}_\pi$  hits a proton in the  $^{28}\text{Si}$  target in the state  $\psi_P$  and emerges in the final state as kaon  $K^+$  moving in the direction  $\hat{\mathbf{k}}_K$  with energy  $E_K$ , whereas the hit proton emerges in the final state as a  $\Sigma^-$  hyperon with momentum  $\mathbf{k}_\Sigma$ . We apply the simple impulse approximation described in [14], with  $K^+$  and  $\pi^-$  plane waves, and obtain:

$$d^3\sigma/d\hat{\mathbf{k}}_\Sigma d\hat{\mathbf{k}}_K dE_K \sim \left| \int d\mathbf{r} \exp(-i\mathbf{q}\cdot\mathbf{r}) \psi_{\Sigma, \mathbf{k}_\Sigma}(\mathbf{r})^{(-)*} \psi_P(\mathbf{r}) \right|^2, \quad (1)$$

where the momentum transfer  $\mathbf{q} = \mathbf{k}_K - \mathbf{k}_\pi$ , and  $\psi_{\Sigma, \mathbf{k}_\Sigma}(\mathbf{r})^{(-)}$  is the  $\Sigma$  scattering wave function which is the solution of the s.p. Schrödinger equation with the s.p. potential

$$U_\Sigma(r) = (V_\Sigma - iW_\Sigma)\theta(R - r), \quad (2)$$

where for  $V_\Sigma$  and  $W_\Sigma$  we use the nuclear matter results discussed in Sec. 2, calculated at  $\rho = n/[(4\pi/3)R^3]$ , where  $n = 27$  is the number of nucleons in the final state.

For the  $^{28}\text{Si}$  target nucleus we assume a simple shell model with a square well s.p. potential  $V_P(r)$  (which determines  $\psi_P$ ) with the radius  $R_P$  (and with a spin-orbit term). The parameters of  $V_P(r)$  are adjusted to the proton separation energies (in particular  $R_P = 3.756$  fm). For  $R$  we make the simple and plausible assumption:  $R = R_P$ .

In the inclusive KEK experiments [12, 13] only the energy spectrum of kaons at fixed  $\hat{\mathbf{k}}_\Sigma$  was measured. To obtain this energy spectrum, we have to integrate the cross-section (1) over  $\hat{\mathbf{k}}_\Sigma$ .

---

<sup>3</sup> Notice that the positive sign of the measured values of  $\varepsilon$  requires an attractive  $\Sigma$  potential at the nuclear surface, *i.e.* at low densities.

We present our results for the inclusive cross-section as a function of  $B_\Sigma$ , the separation (binding) energy of  $\Sigma$  from the hyper nuclear system produced. Our model F and D results<sup>4</sup> for kaon spectrum from  $(\pi^-, K^+)$  reaction on  $^{28}\text{Si}$  at  $\theta_K = 6^\circ$  at  $p_\pi = 1.2 \text{ GeV}/c$  are shown in Fig. 3. We see that the best fit to the data points is obtained for  $V_\Sigma$  derived from model F and with  $W_\Sigma = W_t = W_c + W_e$ . The fit would improve if we considered the distortion of kaon and especially of pion waves (it was noticed already in Ref. [12] that this distortion pushes the kaon spectrum down). Inclusion into the absorptive potential of the contribution  $W_e$  of the elastic  $\Sigma N$  scattering is essential for obtaining this result with  $V_\Sigma$  (model F) = 17.25 MeV. Earlier estimates of the kaon spectrum without this contribution suggested a repulsive  $V_\Sigma$  with an unexpected strength of about 100 MeV. Notice that the action of the absorptive potential  $W_\Sigma$  on the  $\Sigma$  wave function (decrease of this wave function) is similar as the action of a repulsive  $V_\Sigma$ . Therefore, we achieve with strong absorption the same final effect with a relatively weaker repulsion.

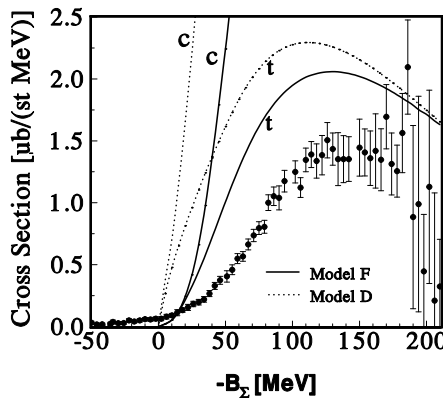


Fig. 3. Kaon spectrum from  $(\pi^-, K^+)$  reaction on  $^{28}\text{Si}$  at  $\theta_K = 6^\circ$  at  $p_\pi = 1.2 \text{ GeV}/c$  obtained with  $V_\Sigma$  determined by models F and D of the  $\Sigma N$  interaction. Curves denoted by  $c(t)$  were obtained with  $W_\Sigma = W_c(W_t)$ . Data points are taken from [13].

## 5. The strangeness exchange reactions

First observations of the strangeness exchange ( $K^-, \pi$ ) reactions with a reliable accuracy were performed at BNL. Here, we shall discuss the  $(K^-, \pi^+)$  reaction observed at BNL on  $\text{Be}^9$  target with  $600 \text{ MeV}/c$  kaons [15].

<sup>4</sup> The remaining models SC and NSC are similar to model D: they all lead to attractive  $V_\Sigma$  in contradistinction to model F leading to repulsive  $V_\Sigma$  (at densities inside nuclei — see Fig. 1). Consequently, the results for the kaon spectrum for models SC and NSC are expected to be similar as in the case of model D.

Proceeding similarly as in the case of the associated production described in Sec. 4, we get the results shown in Fig. 4. We see that similarly as in Sect. 4 the fit to the data points obtained for  $V_\Sigma$  derived from model F is much better than the fit obtained with model D.

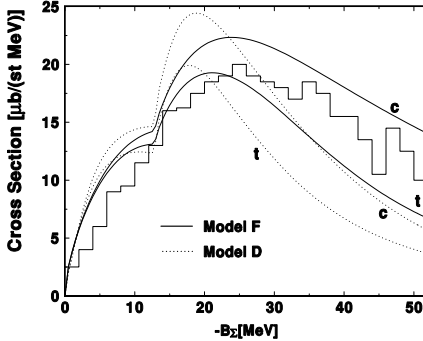


Fig. 4. Pion spectrum from  $(K^-, \pi^+)$  reaction on  ${}^9\text{Be}$  at  $\theta_\pi = 4^\circ$  at  $p_K = 0.6 \text{ GeV}/c$  obtained with  $V_\Sigma$  determined by models F and D of the  $\Sigma N$  interaction. Curves denoted by  $c(t)$  were obtained with  $W_\Sigma = W_c(W_t)$ . Data points are taken from [15].

## 6. Conclusions

- The real part  $V_\Sigma$  of the  $\Sigma$  optical potential is repulsive inside the nucleus and has a shallow attractive pocket at the nuclear surface.
- Among the Nijmegen models of the baryon–baryon interaction only model F leads to this form of  $V_\Sigma$ .
- The contribution of the elastic  $\Sigma N$  scattering to the absorptive part  $W_\Sigma$  of the  $\Sigma$  optical potential is essential in the analysis of  $\Sigma$  production processes.

This research was partly supported by the Polish Ministry of Science and Higher Education under the Research Project No. N N202 046237.

## REFERENCES

- [1] N.M. Nagels, T.A. Rijken, J.J. de Swart, *Phys. Rev.* **D12**, 744 (1975); **D15**, 2547 (1977).
- [2] N.M. Nagels, T.A. Rijken, J.J. de Swart, *Phys. Rev.* **D20**, 1633 (1979).
- [3] P.M.M. Maessen, T.A. Rijken, J.J. de Swart, *Phys. Rev.* **C40**, 2226 (1989); *Nucl. Phys.* **A547**, 245c (1992).
- [4] T.A. Rijken, V.G.J. Stoks, Y. Yamamoto, *Phys. Rev.* **C59**, 21 (1999).

- [5] Y. Yamamoto, T. Motoba, H. Himeno, K. Ikeda, S. Nagata, *Progr. Theor. Phys., Suppl.* **117**, 361 (1994).
- [6] J. Dąbrowski, *Acta Phys. Pol. B* **36**, 3063 (2005).
- [7] T. Nagae *et al.*, *Phys. Rev. Lett.* **80**, 1605 (1998).
- [8] T. Harada *et al.*, *Nucl. Phys. A* **507**, 715 (1990); T. Harada, Y. Akaishi, *Progr. Theor. Phys.* **96**, 145 (1996); T. Harada, *Phys. Rev. Lett.* **81**, 5287 (1998).
- [9] J. Dąbrowski, *Phys. Rev. C* **60**, 025205 (1999).
- [10] J. Dąbrowski, J. Rożynek, *Phys. Rev. C* **78**, 037601 (2008).
- [11] J. Dąbrowski, J. Rożynek, G.S. Anagnostatos, *Eur. Phys. J. A* **14**, 125 (2002).
- [12] H. Noumi *et al.*, *Phys. Rev. Lett.* **89**, 072301 (2002).
- [13] P.K. Saha *et al.*, *Phys. Rev. C* **70**, 044613 (2004).
- [14] J. Dąbrowski, J. Rożynek, *Acta Phys. Pol. B* **35**, 2303 (2004).
- [15] S. Bart *et al.*, *Phys. Rev. Lett.* **83**, 5238 (1999).